amplitudes. If SU(3) interaction symmetry is assumed also, there are only two solutions for the interaction ratios; in each of these all the ratios are determined. Data on the $N \to \Sigma$ processes are in strong contradiction to both these solutions.

Clearly, if the linear-zero postulate were not applied to any amplitude, the SU(3) violation would be less clear-cut. This is because the data analyzed by Odorico contain experimental uncertainties, so that if no supplementary postulate were used, the $N \to \Sigma$ predictions would not be so precise. The significant thing about our results is not the SU(3) violation, but the experimental suggestion that nature prefers the less-well-known linear-zero postulate to SU(3) symmetry for spin-independent amplitudes. More data and phase-shift analyses of the $\bar{K}N \to \pi\Sigma$ and $\pi N \to K\Sigma$ amplitudes are needed to test this suggestion more thoroughly.

---

*Work supported in part by the U. S. Atomic Energy Commission.

[1]R. Odorico, Phys. Lett. 41B, 339 (1972).

[2]R. Odorico, Nucl. Phys. B37, 509 (1972).

[3]R. Odorico, Phys. Lett. 38B, 37 (1972).

[4]R. H. Capps, Phys. Rev. D 7, 3394 (1973).

[5]In Ref. 1, it is stated that the linear-zero assumption (together with the other assumptions of Sec. II B of the present paper) is consistent with t-channel SU(3) if SU(3) is not applied in the s or u channels. This is incorrect, as shown by the argument given here.

[6]Daniel F. Kane, Jr., Phys. Rev. D 5, 1583 (1972).

[7]W. Langbein and F. Wagner, Nucl. Phys. B53, 251 (1973).

[8]R. Odorico, in *Baryon Resonances—73* (Purdue Univ. Press, West Lafayette, Indiana, 1973), pp. 135–147. In this reference, the $\bar{K}N \to \pi\Sigma$ residue ratios are averages over several phase-shift analyses, and are shown in Fig. 6. This is a more up-to-date version of Fig. 2 of Ref. 1.

[9]S. Almehed and C. Lovelace, Nucl. Phys. B40, 157 (1972).

PHYSICAL REVIEW D VOLUME 9, NUMBER 9 1 MAY 1974

Physical trajectories in an inclusive dual resonance model*

J. Randa†
Physics Department, University of Illinois at Urbana-Champaign, Urbana, Illinois 61801
(Received 3 December 1973)

Previous work on the dual resonance model in inclusive vector-meson production is extended to include both abnormally coupled trajectories and trajectories with positive intercept. Differential cross sections and density-matrix elements are obtained and compared to those of the previous calculation. The single-particle spectrum for spinless mesons is also obtained and compared with earlier results.

I. INTRODUCTION AND NOTATION

A. Introduction

In a previous paper[1] the predictions of a standard dual resonance model (DRM) for inclusive vector-meson production were obtained. The calculation had two major shortcomings which one could expect to overcome within the framework of a DRM. The first is that the B_8 which was used[2] contains only normal [for $1+2 \to 3$, $\eta_3 = \eta_1\eta_2$, where $\eta_i = (-1)^{J_i}P_i$] couplings. Consequently, for $\pi N \to \rho X$, where X is anything, only π exchange is included in the t ($\pi\bar{\rho}$) channel. But at very high energies one would expect A_2 exchange to become increasingly important (due to its higher intercept), and we would therefore like to include abnormally coupled trajectories in the calculation. The second unpleasant feature was the use of only one internal trajectory, the "π-ρ" trajectory $\alpha(s) = -m_\pi^2 + s$. While this is not expected to be a fatal flaw, it is desirable to investigate the predictions of a more "physical" model, for the sake of comparison to both experiment and to the predictions of the simpler model.

In this paper we remedy these two ills. Using the kinematic superstructures of Canning and Jacobs,[3] we construct an amplitude with abnormal coupling to accommodate the A_2 trajectory. Provision for trajectories with positive intercepts is made by using the tachyon-free amplitude of Rittenberg and Rubenstein.[4] The one-particle spectra and density matrices of π and A_2 exchange are compared, and the effects (if any) of including positive-intercept trajectories are examined. This latter comparison should provide some indication of whether inclusive predictions made with a simple DRM, such as that used in Ref. 1, contain all the basic features of more detailed models. In this connection, we also calculate the one-particle spectrum for spinless mesons using an amplitude with physical trajectories.

The body of the paper divides roughly into three major sections. In the first part, an eight-point amplitude with the A_2 in three-pion channels is obtained, and then used to calculate cross sections and density-matrix elements. In the second part (Secs. III and IV) we do the same for pions in the three-pion channels. (In both cases, trajectories have physical intercepts, 0.5 for the ρ and A_2 and $-m_\pi^2$ for the π.) Finally, in Sec. V, we compare the results of the two calculations to each other and to previous calculations and discuss our findings.

B. Notation

The notation is essentially that of Ref. 1. For $a+b \to x+X$ we define the usual invariants

$$s=(p_a+p_b)^2, \quad t=(p_a-p_x)^2, \quad u=(p_b-p_x)^2 \,, \qquad (1.1)$$
$$M^2=p_X{}^2=(p_a+p_b-p_x)^2, \quad s'=(p_a+p_x)^2 \,.$$

We also use

$$\alpha_{ab}=\alpha((p_a+p_b)^2),$$
$$\alpha_{a\bar{x}}=\alpha((p_a+p_{\bar{x}})^2) \qquad (1.2)$$
$$=\alpha((p_a-p_x)^2) \,,$$

etc., and let $\alpha \equiv \alpha(M^2)$.

In dealing with the antisymmetric tensor $\epsilon^{\mu\nu\rho\sigma}$, we use the less cumbersome notation

$$\epsilon^{\mu\nu\rho\sigma} p_{1\mu} p_{2\nu} p_{3\rho} p_{4\sigma} = \epsilon^{\cdot\cdot\cdot\cdot} p_1^\cdot p_2^\cdot p_3^\cdot p_4^\cdot \,. \qquad (1.3)$$

II. AMPLITUDE WITH ABNORMAL COUPLING

A. Obtaining the amplitude

Since the A_2, ρ, and π have spin-parity 2^+, 1^-, 0^-, respectively, the $\rho\pi A_2$ coupling is essentially different from the $\rho\pi\pi$ coupling. The $\rho\pi\pi$ coupling is normal, whereas the A_2 couples abnormally to the $\rho\pi$ system. The standard DRM N-particle amplitude includes only normally coupled trajectories.[5] One way to introduce abnormal couplings is to multiply the B_N by a factor (called the superstructure) constructed of $\epsilon^{\mu\nu\rho\sigma}$'s and external momenta. Then, since this factor affects asymptotic behavior due to the dependence on momenta, the trajectories in the B_N are altered in such a way as to preserve the proper asymptotic behavior. Bardakci and Ruegg used this method on the five-point amplitude.[6] Abnormal coupling in the six-point amplitude was studied by Dorren *et al.*,[7] and in the six and eight-point amplitudes by Canning and Jacobs.[3]

There are two ways to determine the amount by which each trajectory in B_N must be lowered in order to maintain proper asymptotic behavior. One way, used by Dorren *et al.*,[7] is to write the superstructure in terms of the invariants of the problem, imposing the constraint that the Gram determinant vanish. The behavior of the superstructure is then studied in all the Regge limits, and trajectories in the B_N are depressed by whatever amount is necessary to ensure leading Regge behavior in all channels.

For large N (>6) this method becomes unwieldy. An alternative method that was proposed by Canning and Jacobs[3] is more suitable for use in our work with eight-point amplitudes. Rather than consider the asymptotic behavior of the superstructure in each Regge limit, they consider the spin structure at the first resonance in each channel. That this method automatically yields proper leading Regge behavior may seem somewhat magical at first, but is due to the fact that the angular momentum in one channel determines the limiting behavior in the dual (crossed) channel.

The spin structure of the superstructure in a certain channel is determined by its transformation properties under O(3) in the channel's rest frame. As a simple example we consider

$$\epsilon^{\mu\cdot\cdot\cdot} p_1^\cdot p_2^\cdot p_3^\cdot \epsilon^{\mu\cdot\cdot\cdot} p_4^\cdot p_5^\cdot p_6^\cdot B_8(\alpha_{12}, \alpha_{13}, \alpha_{14}, \alpha_{15}, \alpha_{16}, \alpha_{23}, \alpha_{24}, \alpha_{25}, \alpha_{26}, \alpha_{27}, \alpha_{34}, \alpha_{35}, \alpha_{36}, \alpha_{37}, \alpha_{45}, \alpha_{46}, \alpha_{47}, \alpha_{56}, \alpha_{57}, \alpha_{67}). \qquad (2.1)$$

(For further examples and full development see Ref. 3.) The dot notation indicates that the p's are contracted into the $\epsilon^{\mu\nu\rho\sigma}$ in the order they occur. At $\alpha_{12}=0$ there is no spin structure in the 12 channel from the B_8. The superstructure can be written

$$Q_\nu P_\rho \epsilon^{\mu\nu\rho\cdot} p_3^\cdot \epsilon^{\mu\cdot\cdot\cdot} p_4^\cdot p_5^\cdot p_6^\cdot \,, \qquad (2.2)$$

where

$$P^\mu = (p_1 + p_2)^\mu \ ,$$
$$Q^\mu = \tfrac{1}{2}(p_1 - p_2)^\mu \ . \tag{2.3}$$

Since Q^μ transforms as a vector and P^μ as a scalar in the 12 rest frame, the superstructure describes production and decay of a spin-one object. If particles 1 and 2 are both 0^- mesons, it is a 1^- meson. As it stands then, expression (2.1) leads to a spin-one resonance in the 12 channel at $\alpha_{12}=0$. By lowering the α_{12} trajectory by one unit $[B_8(\alpha_{12},\ldots) \to B_8(\alpha_{12}-1,\ldots)]$, we remedy this. The spin-one pole now occurs at $\alpha_{12}=1$. (There is no $\alpha_{12}=0$ pole.) This analysis is then repeated for each of the trajectories appearing as arguments of the B_8. The amount by which α_{ij} is lowered is denoted m_{ij}.

A further complication arises due to parity doubling. It is quite possible that in some channel the superstructure will contain both parities for the leading spin present. [In the 24 channel, for example, expression (2.1) has both 2^+ and 2^- pieces.] To ensure leading trajectories of definite parity we depress such channels—we use $(\alpha_{24}-3)$ rather than the $(\alpha_{24}-2)$ needed to give leading behavior.

We now construct our eight-point amplitude. We require that the amplitude "cover" all possible Feynman tree graphs for eight external particles. The amplitude covers a tree graph if it covers each of the graph's resonant channels. A channel is covered if in that channel the amplitude has a leading Regge trajectory of definite naturality, provided the first physical resonance in that channel has not been eliminated by our program of maintaining proper asymptotic behavior (by lowering certain trajectories). For example, in a channel with negative G parity and unnatural parity we require the presence of a spin-zero pole (the π) in our amplitude. For natural parity, positive G parity, we require a spin-one pole (the ρ), but do not require a spin-zero pole. There is one other consideration which we use to simplify matters somewhat. We intend to use the amplitude we develop to study inclusive ρ production at large incident momentum and missing mass squared. We can therefore use the fact that only certain orderings of external particles contribute in our limit,[8] and that we have resonant ρ's in two dipion channels to limit the tree graphs we need cover to those having resonances in the 12 or 23 channel and the 67 or 78 channel.

The next step then is to analyze the 23 superstructures of Ref. 3(b) to see which tree graphs each covers. Having done so, we choose a set of superstructures which will cover all the tree graphs with resonances in the 12 or 23 channel and the 67 or 78 channel. The set we choose is com-

TABLE I. Results of the analysis of the four superstructures used in the amplitude for abnormal coupling.

	$K_3(1,2)$				$K_{10}(1,2)$				$K_{22}(1,2)$				$K_{23}(1,2)$			
Channel	Starting point	m_{ij}	Trajectory	Covered?	Starting point	m_{ij}	Trajectory	Covered?	Starting point	m_{ij}	Trajectory	Covered?	Starting point	m_{ij}	Trajectory	Covered?
12	1^-	1	ρ	Yes	1^-	1	ρ	Yes	1^-	1	ρ	Yes	1^-	1	ρ	Yes
13	1^-	1	A_2	Yes	1^-	1	A_2	Yes	1^-	1	A_2	Yes	1^-	1	A_2	Yes
14	1^+	1	B	Yes	1^+	1	B	Yes	1^-	1	ρ	Yes	1^-	1	ρ	Yes
15	1^-	1	A_2	Yes	1^{+-}	2	π,A_2	No	1^-	1	A_2	Yes	2^{+-}	3	π,A_2	No
16	1^-	1	ρ	Yes	1^-	1	ρ	Yes	1^-	1	ρ	Yes	2^+	2	ρ	No
23	1^-	1	ρ	Yes	1^-	1	ρ	Yes	1^-	1	ρ	Yes	1^-	1	ρ	Yes
24	2^+	2	A_2	Yes	1^{+-}	2	π,A_2	No	2^{+-}	3	π,A_2	No	2^{+-}	3	π,A_2	No
25	2^-	2	B	No	2^{+-}	3	ρ,B	No	3^{+-}	4	ρ,B	No	4^{+-}	5	ρ,B	No
26	2^{+-}	3	π,A_2	No	2^{+-}	3	π,A_2	No	4^{+-}	5	π,A_2	No	4^{+-}	5	π,A_2	No
27	2^+	2	ρ	No	1^-	1	ρ	Yes	4^+	4	ρ	No	3^-	3	ρ	No
34	2^+	2	ρ	No	1^-	1	ρ	Yes	2^+	2	ρ	No	2^+	2	ρ	No
35	2^{+-}	3	π,A_2	No	2^-	2	π	No	3^{+-}	4	π,A_2	No	4^{+-}	5	π,A_2	No
36	2^{+-}	3	ρ,B	No	2^{+-}	3	ρ,B	No	4^{+-}	5	ρ,B	No	4^{+-}	5	ρ,B	No
37	2^{+-}	3	π,A_2	No	1^{+-}	2	π,A_2	No	4^{+-}	5	π,A_2	No	3^{+-}	4	π,A_2	No
45	1^-	1	ρ	Yes	1^-	1	ρ	Yes	2^+	2	ρ	No	3^-	3	ρ	No
46	2^-	2	π	No	1^{+-}	2	π,A_2	No	3^{+-}	4	π,A_2	No	3^{+-}	4	π,A_2	No
47	2^-	2	B	No	1^+	1	B	Yes	3^{+-}	4	ρ,B	No	2^{+-}	3	ρ,B	No
56	1^-	1	ρ	Yes	1^-	1	ρ	Yes	2^+	2	ρ	No	1^-	1	ρ	Yes
57	1^{+-}	2	π,A_2	No	1^-	1	A_2	Yes	2^{+-}	3	π,A_2	No	1^-	1	A_2	Yes
67	1^-	1	ρ	Yes	1^-	1	ρ	Yes	1^-	1	ρ	Yes	1^-	1	ρ	Yes

prised of

$$K_3(1,2)=\epsilon^{\cdot\cdot\cdot\cdot} p_1^{\cdot} p_2^{\cdot} p_3^{\cdot} p_4^{\cdot} \epsilon^{\cdot\cdot\cdot\cdot} p_5^{\cdot} p_6^{\cdot} p_7^{\cdot} p_8^{\cdot}\ ,$$
$$K_{10}(1,2)=\epsilon^{\mu\cdot\cdot\cdot} p_1^{\cdot} p_2^{\cdot} p_3^{\cdot} \epsilon^{\mu\cdot\cdot\cdot} p_5^{\cdot} p_6^{\cdot} p_7^{\cdot}\ ,$$
$$K_{22}(1,2)=\epsilon^{\mu\cdot\cdot\cdot} p_1^{\cdot} p_2^{\cdot} p_3^{\cdot} \epsilon^{\mu\nu\cdot\cdot} p_{13}^{\cdot} p_{58}^{\cdot} \times \epsilon^{\nu\sigma\cdot\cdot} p_{14}^{\cdot} p_{68}^{\cdot} \epsilon^{\sigma\cdot\cdot\cdot} p_6^{\cdot} p_7^{\cdot} p_8^{\cdot}\ , \tag{2.4}$$
$$K_{23}(1,2)=\epsilon^{\mu\cdot\cdot\cdot} p_1^{\cdot} p_2^{\cdot} p_3^{\cdot} \epsilon^{\mu\nu\cdot\cdot} p_{13}^{\cdot} p_{58}^{\cdot} \times \epsilon^{\nu\sigma\cdot\cdot} p_{14}^{\cdot} p_{57}^{\cdot} \epsilon^{\sigma\cdot\cdot\cdot} p_5^{\cdot} p_6^{\cdot} p_7^{\cdot}\ ,$$

and the permuted forms $K_3(4,5), K_3(6,7), K_3(3,4)$, $K_3(8,1), K_3(6,5), K_3(1,8), K_3(8,7), K_3(3,2), K_3(5,6)$, $K_{10}(8,7), K_{10}(8,1), K_{10}(3,4), K_{10}(6,5), K_{10}(1,8)$, $K_{22}(8,1), K_{22}(5,6), K_{23}(7,6), K_{23}(8,7), K_{23}(2,3)$. The numbers in parentheses following the K's indicate the first two momenta to be contracted into the first ϵ. The other momentum subscripts follow in either increasing or decreasing order, depending upon whether the numbers in parentheses increased or decreased. For example,

$$K_{10}(6,5)=\epsilon^{\mu\cdot\cdot\cdot} p_6^{\cdot} p_5^{\cdot} p_4^{\cdot} \epsilon^{\mu\cdot\cdot\cdot} p_2^{\cdot} p_1^{\cdot} p_8^{\cdot}\ . \tag{2.5}$$

The behaviors of the superstructures of Eq. (2.4) are given in Table I.

The presence of the B trajectories $[I^G=1^+$, $P=(-1)^{J+1}$, $C=(-1)^J]$ in certain channels may seem undesirable at first since it is not one of the leading meson trajectories. However, since in our work the subenergy of these channels is large, the low intercept of the B trajectory should not matter. The trajectories for the various channels were dictated by our intention to use this amplitude in studying $\pi^- p \to \rho^0 X$. Our choice of a set of superstructures covering all the necessary tree graphs is not unique. In choosing superstructures, any which would require elimination of tachyons were discarded. This was a matter of taste; we felt it desirable to avoid any such complications which were not strictly necessary. After imposition of this criterion, from the remaining superstructures those covering the most tree graphs were chosen.

We are now almost ready to add up all the terms to get the amplitude. Before we can, however, we must face one more question: With what coefficients do we add the terms? The ratios of the coefficients of various superstructures will determine the relative amounts of different couplings of internal trajectories. Since our interest does not lie in different internal couplings, we make all coefficients equal to unity (to within a sign). The effect of changing the coefficients will be considered later. The sign preceding each superstructure is determined by positivity conditions on the residue at the multiple pole $1+2+3+4 \to A+3+4 \to B+4 \to C \to B+4 \to A+3+4 \to 1+2+3+4$. The final consideration is that we want our amplitude to be invariant under inversion of the ordering of the external particles $[F(1,2,3,\ldots)=F(8,7,6,\ldots)]$. The ambiguity of whether to count symmetric terms (K_{22}'s) twice is lumped with the coefficient question.

The amplitude we use is then

$$F(1,2,3,4,5,6,7,8)=F_0(1,2,3,4,5,6,7,8)+F_0(8,7,6,5,4,3,2,1)\ , \tag{2.6}$$

where

$$F_0(1,2,3,4,5,6,7,8)=[F_3(1,2)+F_3(3,4)+F_3(4,5)+F_3(5,6)+F_3(6,7)+F_3(8,1)]+[F_{10}(1,2)+F_{10}(3,4)+F_{10}(8,1)] + \tfrac{1}{2}[F_{22}(1,2)+F_{22}(5,6)+F_{22}(8,1)]-[F_{23}(1,2)+F_{23}(2,3)]\ , \tag{2.7}$$

and

$$F_3(i,i+1)=K_3(i,i+1)\,B_8(\alpha_{12}-m_{j,j+1},\ \alpha_{13}-m_{j,j+2},\ \ldots,\ \alpha_{23}-m_{j+1,j+2},\ \ldots),\quad j=2-i \mod 8 \tag{2.8}$$

$$F_3(i,i-1)=K_3(i,i-1)\,B_8(\alpha_{12}-m_{k,k+1},\ \alpha_{13}-m_{k-1,k+1},\ \ldots,\ \alpha_{23}-m_{k-1,k},\ \alpha_{24}-m_{k-2,k},\ \ldots)\ ,\quad k=1-j=-1-i \mod 8 \tag{2.9}$$

and similarly for the other superstructures, where the m_{ij} are read off from Table I. For example,

$$F_{23}(7,6)=\epsilon^{\mu\cdot\cdot\cdot} p_7^{\cdot} p_6^{\cdot} p_5^{\cdot} \epsilon^{\mu\nu\cdot\cdot} p_{57}^{\cdot} p_{83}^{\cdot} \epsilon^{\nu\sigma} p_{47}^{\cdot} p_{13}^{\cdot} \epsilon^{\sigma\cdot\cdot\cdot} p_3^{\cdot} p_2^{\cdot} p_1^{\cdot} \times B_8(\alpha_{12}-1,\ \alpha_{13}-1,\ \alpha_{14}-3,\ \alpha_{15}-4,\ \alpha_{16}-3,\ \alpha_{23}-1,\ \alpha_{24}-4,\ \alpha_{25}-5,\ \alpha_{26}-5,\ \alpha_{27}-2,\ \alpha_{34}-3,\ \alpha_{35}-5,\ \alpha_{36}-5,\ \alpha_{37}-3,\ \alpha_{45}-2,\ \alpha_{46}-3,\ \alpha_{47}-1,\ \alpha_{56}-1,\ \alpha_{57}-1,\ \alpha_{67}-1)\ . \tag{2.10}$$

The factor of $\frac{1}{2}$ preceding the F_{22} terms in Eq. (2.6) is to ensure in the total amplitude a coefficient of 1 for the F_{22} terms, which are symmetric under inversion of external ordering.

B. Calculation

Now that we have an eight-point amplitude with abnormally coupled trajectories, we can follow the

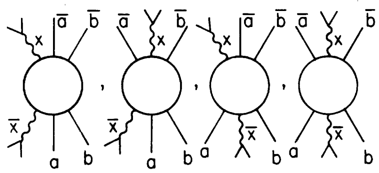

FIG. 1. The four DRM diagrams which contribute to $a+b \to x+X$ in the fragmentation region of a.

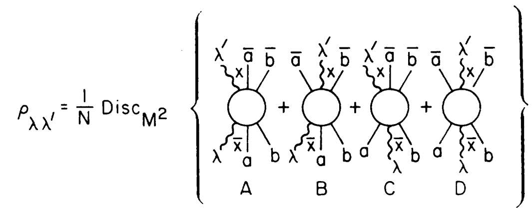

FIG. 2. Diagrammatic representation of density-matrix elements.

procedure used in Ref. 1 to obtain expressions for inclusive ρ-production cross sections and the density matrix due to A_2 exchange. For $a+b \to x+X$, where for our case x is a vector meson, we know in the limit $s, M^2 \to \infty$, small t that we only need to keep certain orderings of external particles in our eight-point function. The graphs we need to consider are shown in Fig. 1. The density matrix elements are computed from Fig. 2, where

$$N = \sum_{\lambda} \mathrm{Disc}_{M^2} \langle ab\bar{x}(\lambda) | T | ab\bar{x}(\lambda)\rangle \tag{2.11}$$

and

$$\frac{1}{\sigma_{ab}} E_x \frac{d^3\sigma}{dp_x{}^3} = \frac{\Gamma(\alpha_{\mathrm{vac}}+1)}{\pi(\alpha_{ab})^{\alpha_{\mathrm{vac}}}} N \,. \tag{2.12}$$

The next step is to calculate A, B, C, and D in the manner of Ref. 1. For A, we first take the residue at the $\alpha_{12} = \alpha_{16} = 1$ pole. This gives us the first graph of Fig. 1, with the propagator denominators for x and $\bar{x}$ removed. It contains contributions from the spin-zero daughter of the ρ in both x and $\bar{x}$ channels. We eliminate these and factor off the $\rho\pi\pi$ vertices (as explained in detail in Ref. 1) and are left with our expression for A:

$$\begin{aligned} A = {} & \epsilon^{\mu\cdots}\epsilon^{\cdot}\, p_{\bar{x}}^{\cdot} p_a^{\cdot}\, \epsilon_{\mu}^{\mu\nu\cdot\cdot}\, p_{a\bar{x}}^{\cdot} p_{\bar{b}}^{\cdot}\, \epsilon^{\nu\sigma\cdot\cdot}\, p_b^{\cdot} p_{\bar{a}x}^{\cdot}\, \epsilon^{\sigma\cdots}\, p_a^{\cdot} p_x^{\cdot}\, \epsilon'^{*\cdot} \\ & \times\{B_6(\alpha^A_{a\bar{x}}-1,\ \alpha^{\rho}-1,\ \alpha^A_{\bar{a}x}-1,\ \alpha^{\rho}_{ab}-2,\ \alpha^{v}_{b\bar{b}}-1,\ \alpha^{\rho}_{\bar{a}\bar{b}}-2,\ \alpha^{\pi}_{ab\bar{b}}-3,\ \alpha^{\pi}_{\bar{a}b\bar{b}}-3,\ \alpha^{v}_{x\bar{x}}-4) \\ & \quad - B_6(\alpha^A_{a\bar{x}}-1,\ \alpha^{\rho}-2,\ \alpha^A_{\bar{a}x}-1,\ \alpha^{\rho}_{ab}-2,\ \alpha^{v}_{b\bar{b}}-1,\ \alpha^{\rho}_{\bar{a}\bar{b}}-2,\ \alpha^{\pi}_{ab\bar{b}}-3,\ \alpha^{\pi}_{\bar{a}b\bar{b}}-3,\ \alpha^{v}_{x\bar{x}}-4)\} \\ & + \epsilon^{\mu\cdots}\, p_{\bar{x}}^{\cdot} p_a^{\cdot}\, \epsilon^{\cdot}\, \epsilon^{\mu\cdots}\, p_{\bar{b}}^{\cdot} p_{\bar{a}}^{\cdot}\, \epsilon'^{*\cdot}\, B_6(\alpha^A_{a\bar{x}}-1,\ \alpha^{B}-1,\ \alpha^A_{\bar{a}x}-2,\ \alpha^{\rho}_{ab}-1,\ \alpha^{v}_{b\bar{b}}-1,\ \alpha^{\rho}_{\bar{a}\bar{b}}-1,\ \alpha^{\pi}_{ab\bar{b}}-2,\ \alpha^{\pi}_{\bar{a}b\bar{b}}-2,\ \alpha^{v}_{x\bar{x}}-3) \\ & + \epsilon^{\mu\cdots}\, p_x^{\cdot} p_{\bar{a}}^{\cdot}\, \epsilon'^{*\cdot}\, \epsilon^{\mu\cdots}\, p_b^{\cdot} p_a^{\cdot}\, \epsilon^{\cdot}\, B_6(\alpha^A_{a\bar{x}}-2,\ \alpha^{B}-1,\ \alpha^A_{\bar{a}x}-1,\ \alpha^{\rho}_{ab}-1,\ \alpha^{v}_{b\bar{b}}-1,\ \alpha^{\rho}_{\bar{a}\bar{b}}-1,\ \alpha^{\pi}_{ab\bar{b}}-2,\ \alpha^{\pi}_{\bar{a}b\bar{b}}-2,\ \alpha^{v}_{x\bar{x}}-3), \end{aligned} \tag{2.13}$$

where

$$\epsilon = \epsilon(\lambda), \qquad \epsilon'^{*} = \epsilon(\lambda')^{*} \,. \tag{2.14}$$

The superscripts on the α's indicate which trajectory the superstructure places in that channel. (v is the vacuum trajectory.) The brevity of this expression relative to the corresponding expression in Ref. 1 is due to the spin-one structure in the 12 and 78 channels being contained in the superstructure. Consequently, taking the residue of the B_8 leads to a spin-zero form and not to the proliferation of terms obtained in the earlier case, where the spin-one structure was contained in the B_8. The paucity of terms which appear in the expression for A compared to the number in F is attributable to three causes. Some terms did not have $\alpha_{12}=1$ and $\alpha_{16}=1$ poles and hence could not contribute to A. Some were parity-doubled (and therefore depressed) in the 45 channel, which would lead to them being down by one power of M^2; these were neglected. And finally, many terms went to zero when we went forward, setting $p_{\bar{x}} = -p_x$, etc.

Now, using the results of DeTar, Kang, Tan, and Weiss[8] (DKTW), we can take the discontinuity in M^2 and obtain

$$\begin{aligned} \frac{1}{\pi}\mathrm{Disc}_{M^2} A = {} & \epsilon^{\mu\cdots}\, p_a^{\cdot} p_x^{\cdot}\, \epsilon^{\cdot}\, \epsilon^{\mu\nu\cdot\cdot}\, p_{a\bar{x}}^{\cdot} p_b^{\cdot}\, \epsilon^{\nu\sigma\cdot\cdot}\, p_b^{\cdot} p_{a\bar{x}}^{\cdot}\, \epsilon^{\sigma\cdots}\, p_a^{\cdot} p_x^{\cdot}\, \epsilon'^{*\cdot} \left(\frac{\alpha_\rho(s)-2}{\alpha_\rho(M^2)-1}\right)^{2\alpha_{A_2}(t)-2} \\ & \times DI\left(\frac{\alpha_\rho(M^2)-1}{\alpha_\rho(s)-2},\ \frac{\alpha_\rho(M^2)-1}{\alpha_\rho(s)-2};\ \alpha_A(t)-1,\ \alpha_A(t)-1,\ \alpha_A(t)-1,\ \alpha_A(t)-1,\ -3,\ 0\right) \\ & + [\epsilon^{\mu\cdots}\, p_a^{\cdot} p_x^{\cdot}\, \epsilon^{\cdot}\, \epsilon^{\mu\cdots}\, p_a^{\cdot} p_b^{\cdot}\, \epsilon'^{*\cdot} + \epsilon^{\mu\cdots}\, p_a^{\cdot} p_x^{\cdot}\, \epsilon'^{*\cdot}\, \epsilon^{\mu\cdots}\, p_a^{\cdot} p_b^{\cdot}\, \epsilon^{\cdot}] \left(\frac{\alpha_\rho(s)-1}{\alpha_B(M^2)-1}\right)^{2\alpha_A(t)-3} \\ & \times I\left(\frac{\alpha_B(M^2)-1}{\alpha_\rho(s)-1},\ \frac{\alpha_B(M^2)-1}{\alpha_\rho(s)-1};\ \alpha_A(t)-1,\ \alpha_A(t)-2,\ \alpha_A(t)-1,\ \alpha_A(t)-2,\ -2,\ 0\right) \end{aligned} \tag{2.15}$$

where

$$I(\alpha_1, \beta_1; \alpha_2, \beta_2, \alpha_3, \beta_3, \gamma, \delta) = \int_0^\infty dy_1\, dy_2\, y_1^{-\alpha_2-1}\, y_2^{-\beta_2-1}(1-\alpha_1 y_1)^{\alpha_3}(1-\beta_1 y_2)^{\beta_3} \times (1-\alpha_1 y_1 - \beta_1 y_2)^{\gamma}(1-y_1-y_2)^{\delta}\,\theta(1-y_1-y_2) \tag{2.16}$$

and

$$DI\left(\frac{\alpha}{\alpha_{ab}}, \frac{\alpha}{\alpha_{ab}}; \alpha_2, \beta_2, \alpha_3, \beta_3, \gamma, \delta\right) = I\left(\frac{\alpha}{\alpha_{ab}}, \frac{\alpha}{\alpha_{ab}}; \alpha_2, \beta_2, \alpha_3, \beta_3, \gamma, \delta\right) - \left(\frac{\alpha}{\alpha-1}\right)^{\alpha_2+\beta_2} I\left(\frac{\alpha-1}{\alpha_{ab}}, \frac{\alpha-1}{\alpha_{ab}}; \alpha_2, \beta_2, \alpha_3, \beta_3, \gamma, \delta\right). \tag{2.17}$$

The same procedure is followed for B, C, and D. The expressions obtained are somewhat lengthier and are found in Table II.

C. Numerical evaluation of A_2 exchange

The expression for $\text{Disc}_{M^2}\,(A+B+C+D)$ can now be evaluated numerically, and cross sections and density-matrix elements obtained. The results are summarized in Figs. 3–7. In Fig. 3 the cross section $d\sigma/dt\,dM^2$ is plotted as a function of $t'=(t-t_{\min})$ for large s and various values of M^2/s. (At large s the cross section only depends on the ratio M^2/s and on t.) The forward dip is expected (for a Reggeized A_2) since the A_2 only couples to the $\rho\pi$ system for helicity-one ρ's, and this amplitude is down by a factor of $(1/\cos\theta_t)$ in the forward direction.[9] This dip becomes increasingly dramatic as M^2/s decreases as is expected since $\cos\theta_t$ increases as s/M^2 does. There is no dip-shoulder structure at larger (~ -0.5 GeV$^2/c^2$) t', nor is it expected for A_2 (positive-signature) exchange. Figure 4 shows the dependence of $E_x\, d^3\sigma/dp_x^3$ on $p_{x\perp}$ for fixed $p_{x\parallel}/p_{\text{inc}}$.

The density-matrix element ρ_{1-1} in the Gottfried-Jackson frame is displayed in Fig. 5. The elements ρ_{11} and ρ_{00} are not plotted; they are constant at 0.5 and 0, respectively. For natural-parity exchange in the t channel we expect $\rho_{00}=0$ and $\rho_{11}-\rho_{1-1}=0$ for large $\cos\theta_t$. However, near the forward direction, $\cos\theta_t$ is not large, and ρ_{1-1} is forced by kinematics to be zero at the forward point. Away from this point, $\cos\theta_t$ is large if s/M^2 is large. We see in Fig. 5 that as M^2/s becomes smaller, ρ_{1-1} approaches $\rho_{11}=0.5$.

Another matter worth studying is the contribution of depressed terms. Terms with parity doubling on the t-channel trajectory had this trajectory lowered by one unit. However, since s/M^2 is not necessarily large, we could not neglect these terms. Their size can now be checked numerically. Figure 6 shows the relative size of the pure A_2 versus the parity-doubled parts for particular values of M^2/s. As can be seen, even at rather modest values of s/M^2, the parity-doubled part is negligible except in the very forward direction, and even there it accounts for less than half the cross section.

The effect of varying the coefficients of the terms which went into the full amplitude should now be dealt with. Fortune smiles upon us in this case, and we find that the shape of our results does not depend strongly on these coefficients. This occurs because one term is clearly dominant and also because all the terms have similar t' dependence. Figure 7 demonstrates this, comparing the cross sections for the cases where the coefficient of the dominant term is 5 and then $\frac{1}{5}$, instead of the original choice of 1. The curves are normalized to agree for larger $|t'|$ to facilitate comparison of the shapes.

III. NORMAL COUPLING WITH PHYSICAL TRAJECTORIES

A. Obtaining the amplitude

We now turn to the task of constructing a more physically realistic DRM amplitude for pion exchange in inclusive ρ production. In particular we wish to allow for internal trajectories which are not pion trajectories. We would like the ρ trajectory to have intercept $\frac{1}{2}$, and we would like a vacuum trajectory with intercept 1 in order to simulate Pomeron exchange. However, introduction of trajectories with positive intercepts also introduces the problem of tachyons which must be eliminated.

To handle this difficulty we refer to the paper by Rittenberg and Rubenstein.[4] They attempt to construct amplitudes which have (obey) (a) all the relevant singularities, (b) Regge behavior in all channels, (c) the bootstrap condition, and (d) absence of tachyons. All the "relevant singularities" are poles. Condition (b) is self-explanatory, as is condition (d). The bootstrap condition is that one obtains the $(N-M+1)$-point amplitude when one

TABLE II. Expressions for Disc_{M^2} of the terms B, C, and D for abnormally coupled internal trajectories.

$$\frac{1}{\pi}\mathrm{Disc}_{M^2}(B+C)=B_1+B_2+B_3+B_4$$

$$B_1=-2\epsilon^{\mu\cdots}p_{\dot a}p_{\dot x}\epsilon\cdot\epsilon^{\mu\nu\cdots}p_{\dot a\bar x}p_{\dot b}\epsilon^{\nu\sigma\cdots}p_{\dot b}p_{\dot a\bar x}\epsilon^{\sigma\cdots}p_{\dot a}p_{\dot x}\epsilon'^{*}\cdot\cos[\pi\alpha_A(t)]\left(\frac{\alpha_\rho(s)-2}{\alpha_\rho(M^2)-1}\right)^{\alpha_A(t)-1}\left(-\frac{\alpha_A(u)-3}{\alpha_\rho(M^2)-1}\right)^{\alpha_A(t)-1}$$
$$\times DI\left(\frac{\alpha_\rho(M^2)-1}{\alpha_A(u)-3},\frac{\alpha_\rho(M^2)-1}{\alpha_\rho(s)-2};\alpha_A(t)-1,\alpha_A(t)-1,\alpha_A(t)+\alpha_A(s')-2,\alpha_A(t)+\alpha_A(s')-3,-\alpha_A(s')-1,0\right)$$

$$B_2=[\epsilon^{\mu\cdots}p_{\dot a}p_{\dot x}\epsilon\cdot\epsilon^{\mu\nu\cdots}p_{\dot a}p_{\dot x}\epsilon^{\nu\sigma\cdots}p_{\dot b}p_{\dot x}\epsilon^{\sigma\cdots}p_{\dot b}p_{\dot x}\epsilon'^{*}\cdot e^{-i\pi\alpha_A(t)}+\epsilon^{\mu\cdots}p_{\dot a}p_{\dot x}\epsilon'^{*}\cdot\epsilon^{\mu\nu\cdots}p_{\dot a}p_{\dot x}\epsilon^{\nu\sigma\cdots}p_{\dot b}p_{\dot x}\epsilon^{\sigma\cdots}p_{\dot b}p_{\dot x}\epsilon\cdot e^{i\pi\alpha_A(t)}]$$
$$\times\Bigg[\left(\frac{\alpha_\rho(s)-2}{\alpha_\rho(M^2)-4}\right)^{\alpha_A(t)-3}\left(-\frac{\alpha_A(u)-1}{\alpha_\rho(M^2)-4}\right)^{\alpha_A(t)-5}$$
$$\times DI\left(\frac{\alpha_\rho(M^2)-4}{\alpha_\rho(s)-2},\frac{\alpha_\rho(M^2)-4}{\alpha_A(u)-1};\alpha_A(t)-3,\alpha_A(t)-5,\alpha_A(t)+\alpha_A(s')-4,\alpha_A(t)+\alpha_A(s')-2,-\alpha_A(s')-2,0\right)$$
$$+\left(\frac{\alpha_\rho(s)-4}{\alpha_\rho(M^2)-2}\right)^{\alpha_A(t)-1}\left(\frac{\alpha_A(u)-1}{\alpha_\rho(M^2)-2}\right)^{\alpha_A(t)-4}$$
$$\times DI\left(\frac{\alpha_\rho(M\ )-2}{\alpha_\rho(s)-4},\frac{\alpha_\rho(M^2)-2}{\alpha_A(u)-1};\alpha_A(t)-1,\alpha_A(t)-4,\alpha_A(t)+\alpha_A(s')-3,\alpha_A(t)+\alpha_A(s')-1,-\alpha_A(s')-2,0\right)\Bigg]$$

$$B_3=[\epsilon^{\mu\cdots}p_{\dot x}p_{\dot a}\epsilon'^{*}\cdot\epsilon^{\mu\cdots}p_{\dot a}p_{\dot b}\epsilon\cdot e^{-i\pi\alpha_A(t)}+\epsilon^{\mu\cdots}p_{\dot x}p_{\dot a}\epsilon\cdot\epsilon^{\mu\cdots}p_{\dot a}p_{\dot b}\epsilon'^{*}\cdot e^{i\pi\alpha_A(t)}]\left(\frac{\alpha_\rho(s)-1}{\alpha_B(M^2)-1}\right)^{\alpha_A(t)-2}\left(-\frac{\alpha_A(u)-1}{\alpha_B(M^2)-1}\right)^{\alpha_A(t)-1}$$
$$\times I\left(\frac{\alpha_B(M^2)-1}{\alpha_\rho(s)-1},\frac{\alpha_B(M^2)-1}{\alpha_A(u)-1};\alpha_A(t)-2,\alpha_A(t)-1,\alpha_A(t)+\alpha_A(s')-3,\alpha_A(t)+\alpha_A(s')-2,-\alpha_A(s')-1,0\right)$$

$$B_4=-[\epsilon^{\mu\cdots}p_{\dot a}p_{\dot x}\epsilon\cdot\epsilon^{\mu\cdots}p_{\dot b}p_{\dot x}\epsilon'^{*}\cdot e^{-i\pi\alpha_A(t)}+\epsilon^{\mu\cdots}p_{\dot a}p_{\dot x}\epsilon'^{*}\cdot\epsilon^{\mu\cdots}p_{\dot b}p_{\dot x}\epsilon\cdot e^{i\pi\alpha_A(t)}]\left(\frac{\alpha_\rho(s)-1}{\alpha_B(M^2)-1}\right)^{\alpha_A(t)-1}\left(-\frac{\alpha_A(u)-1}{\alpha_B(M^2)-1}\right)^{\alpha_A(t)-2}$$
$$\times I\left(\frac{\alpha_B(M^2)-1}{\alpha_\rho(s)-1},\frac{\alpha_B(M^2)-1}{\alpha_A(u)-1};\alpha_A(t)-1,\alpha_A(t)-2,\alpha_A(t)+\alpha_A(s')-3,\alpha_A(t)+\alpha_A(s')-2,-\alpha_A(s'),0\right)$$

$$\frac{1}{\pi}\mathrm{Disc}_{M^2}D=D_1+D_2+D_3$$

$$D_1=[\epsilon^{\mu\cdots}p_{\dot a}p_{\dot x}\epsilon\cdot\epsilon^{\mu\cdots}p_{\dot b}p_{\dot x}\epsilon'^{*}\cdot+\epsilon^{\mu\cdots}p_{\dot a}p_{\dot x}\epsilon'^{*}\cdot\epsilon^{\mu\cdots}p_{\dot b}p_{\dot x}\epsilon\cdot]\left(-\frac{\alpha_A(u)-2}{\alpha_B(M^2)-1}\right)^{\alpha_A(t)-1}\left(-\frac{\alpha_A(u)-1}{\alpha_B(M^2)-1}\right)^{\alpha_A(t)-2}$$
$$\times I\left(\frac{\alpha_B(M^2)-1}{\alpha_A(u)-2},\frac{\alpha_B(M^2)-1}{\alpha_A(u)-1};\alpha_A(t)-1,\alpha_A(t)-2,\alpha_A(t)-1,\alpha_A(t),-2,0\right)$$

$$D_2=[\epsilon^{\mu\cdots}p_{\dot b}p_{\dot x}\epsilon\cdot\epsilon^{\mu\nu\cdots}p_{\dot b}p_{\dot x}\epsilon^{\nu\sigma\cdots}p_{\dot x}p_{\dot a}\epsilon^{\sigma\cdots}p_{\dot a}p_{\dot x}\epsilon'^{*}\cdot+\epsilon^{\mu\cdots}p_{\dot b}p_{\dot x}\epsilon'^{*}\cdot\epsilon^{\mu\nu\cdots}p_{\dot b}p_{\dot x}\epsilon^{\nu\sigma\cdots}p_{\dot x}p_{\dot a}\epsilon^{\sigma\cdots}p_{\dot a}p_{\dot x}\epsilon\cdot]$$
$$\times\left(-\frac{\alpha_A(u)-2}{\alpha_\rho(M^2)-2}\right)^{\alpha_A(t)-1}\left(-\frac{\alpha_A(u)-1}{\alpha_\rho(M^2)-2}\right)^{\alpha_A(t)-4}DI\left(\frac{\alpha_\rho(M^2)-2}{\alpha_A(u)-2},\frac{\alpha_\rho(M^2)-2}{\alpha_A(u)-1};\alpha_A(t)-1,\alpha_A(t)-4,\alpha_A(t)-1,\alpha_A(t),-3,0\right)$$

$$D_3=\epsilon^{\mu\cdots}p_{\dot b}p_{\dot x}\epsilon'^{*}\cdot\epsilon^{\mu\nu\cdots}p_{\dot a}p_{\dot b\bar x}\epsilon^{\nu\sigma\cdots}p_{\dot b\bar x}p_{\dot a}\epsilon^{\sigma\cdots}p_{\dot b}p_{\dot x}\epsilon\cdot\left(-\frac{\alpha_A(u)-1}{\alpha_\rho(M^2)-1}\right)^{2\alpha_A(t)-6}$$
$$\times\Bigg[DI\left(\frac{\alpha_\rho(M^2)-1}{\alpha_A(u)-1},\frac{\alpha_\rho(M^2)-1}{\alpha_A(u)-1};\alpha_A(t)-3,\alpha_A(t)-3,\alpha_A(t)-1,\alpha_A(t)-1,-2,0\right)$$
$$-2\left(\frac{\alpha_\rho(M^2)-1}{\alpha_\rho(M^2)-2}\right)^{2\alpha_A(t)-6}DI\left(\frac{\alpha_\rho(M^2)-2}{\alpha_A(u)-1},\frac{\alpha_\rho(M^2)-2}{\alpha_A(u)-1};\alpha_A(t)-3,\alpha_A(t)-3,\alpha_A(t)-1,\alpha_A(t)-1,-2,0\right)$$
$$+\left(\frac{\alpha_\rho(M^2)-1}{\alpha_\rho(M^2)-3}\right)^{2\alpha_A(t)-6}DI\left(\frac{\alpha_\rho(M^2)-3}{\alpha_A(u)-1},\frac{\alpha_\rho(M^2)-3}{\alpha_A(u)-1};\alpha_A(t)-3,\alpha_A(t)-3,\alpha_A(t)-1,\alpha_A(t)-1,-2,0\right)\Bigg]$$

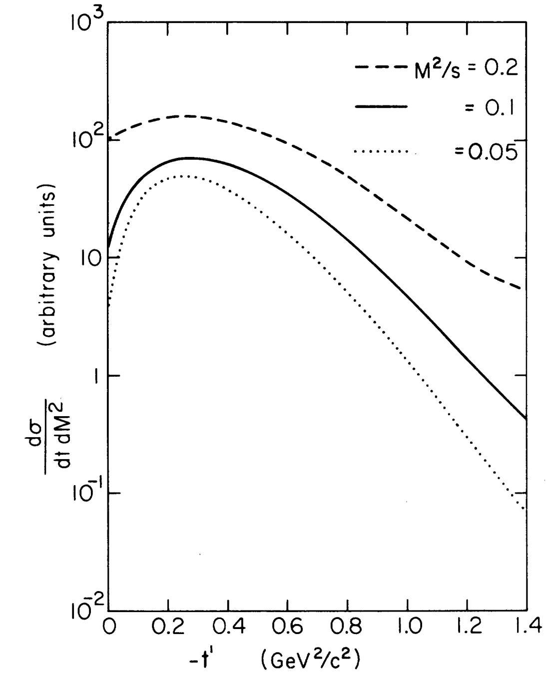

FIG. 3. $d\sigma/dtdM^2$ for A_2 exchange at $M^2/s=0.2$, 0.1, 0.05.

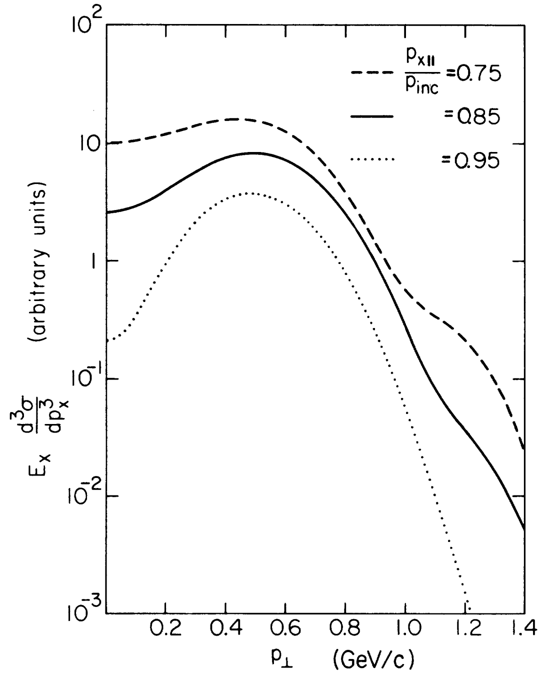

FIG. 4. $E_x d^3\sigma/dp_x^{\,3}$ for A_2 exchange at $p_{x\parallel}/p_i=0.95$, 0.85, 0.75.

evaluates the N-point amplitude at the spin-zero pole in the subenergy of M external particles. The manner in which they approach the problem is to look for generalizations of Lovelace's[10] solution for the four-point case. Standard B_N's are multiplied by factors of α_{ij} to eliminate the tachyons at $\alpha_{ij}=0$. The α's in the B_N are then lowered by amounts (easily determined by the methods of Sec. II) to preserve proper Regge behavior—or, equivalently, spin structure at poles.

The solution found in Ref. 4 for the case of eight external particles is

$$\begin{aligned}F_0=\sum\{&\alpha_{12}\alpha_{45}\alpha_{67}B_8(\alpha_{12},\alpha_{13},\alpha_{14}-1,\alpha_{15},\alpha_{16}-1,\alpha_{23}-1,\alpha_{24}-2,\alpha_{25}-1,\alpha_{26}-2,\alpha_{27}-1,\alpha_{34}-1,\alpha_{35},\alpha_{36}-1,\\&\qquad\alpha_{45},\alpha_{46}-1,\alpha_{47}-1,\alpha_{56}-2,\alpha_{57}-1,\alpha_{67})\\&+\alpha_{14}\alpha_{23}\alpha_{67}B_8(\alpha_{12}-1,\alpha_{13},\alpha_{14},\alpha_{15},\alpha_{16}-1,\alpha_{23},\alpha_{24},\alpha_{25}-1,\alpha_{26}-2,\alpha_{27}-1,\alpha_{34}-1,\alpha_{35}-2,\alpha_{36}-3,\\&\qquad\alpha_{37}-2,\alpha_{45}-1,\alpha_{46}-2,\alpha_{47}-1,\alpha_{56}-1,\alpha_{57},\alpha_{67})\\&-\alpha_{12}\alpha_{34}\alpha_{56}B_8(\alpha_{12},\alpha_{13}-1,\alpha_{14}-1,\alpha_{15}-1,\alpha_{16}-1,\alpha_{23}-2,\alpha_{24}-1,\alpha_{25}-2,\alpha_{26}-1,\alpha_{27}-1,\\&\qquad\alpha_{34},\alpha_{35}-1,\alpha_{36}-1,\alpha_{37},\alpha_{45}-2,\alpha_{46}-1,\alpha_{47}-1,\alpha_{56},\alpha_{57},\alpha_{67}-1)\},\end{aligned}\tag{3.1}$$

where the sum is over all permutations compatible with duality rules. It should be noted that Eq. (3.1) is not fully (all channels) Regge-behaved term by term, but only when all terms are taken together. The negative sign preceding the last term insures that the three terms add in all regions of interest.

Is Eq. (3.1) suitable for use as our eight-point function? Not quite. As it stands, the F_0 so defined is not symmetric under inversion of the order of the external particles. To remedy this, we define

$$\begin{aligned}F&=F_0(1,2,3,\ldots)+F_0(8,7,6,\ldots)\\&=\sum\{F_{\mathrm{I}}+F_{\mathrm{I(inv)}}+2F_{\mathrm{II}}-F_{\mathrm{III}}-F_{\mathrm{III(inv)}}\}\end{aligned}\tag{3.2}$$

where F_{I}, F_{II}, and F_{III} are the first, second, and third terms of Eq. (3.1). The "(inv)" indicates that the ordering of external particles is reversed, and we have noted in writing (3.2) that F_{II} and $F_{\mathrm{II(inv)}}$ are identical.

The amplitude defined by Eq. (3.2) still does not cover (in the sense of Sec. II) all the tree graphs of interest. We are, however, fortunate in both the magnitude and the manner of this failure. Of the 56 tree graphs to be covered, only the three of Fig. 8 are not covered. Also, in each case the failure is expected to be inconsequential. Figure 8(a) would be covered except for the fact that term $F_{\rm I}$ has a ρ trajectory in the 56 channel whose first resonance is at $J^P=2^+$. While this would be sufficient cause for consternation in other kinematic regions, it is not expected to have much effect on our own calculation, where $|s_{56}|$ will always be very large. Similarly, Figs. 8(b) and 8(c) would be covered by $F_{\rm III}$ and $F_{\rm III(inv)}$ except for the lack of the $\alpha_{45}=1$ pole. This does not worry us since the α_{45} trajectory will always be evaluated at $s_{45}=0$ and our amplitude is constructed to have the proper asymptotic behavior in channels dual to the 45 channel. In fact, since we intend to use $\alpha_{45}(0)=1$ to simulate Pomeron exchange, we do not want a pole with spin one. Hence, Eq. (3.2) is quite acceptable from the standpoint of covering tree graphs.

Equation (3.2) will serve as our eight-point amplitude in this section. The results of DKTW regarding which orderings of external particles contribute in our region of interest still apply, since noncontributing orderings are damped exponentially; and consequently the results will not be affected by lowering some trajectories and multiplying by some subenergies. And so we now proceed as in Secs. I and II to compute the cross section and density matrix.

B. Calculation

As before, we must calculate A, B, C, D shown in Fig. 1, now using the F defined in Eq. (3.2) instead of the F of Eq. (2.5). Considering first only A, we see that the terms $F_{\rm III}$ and $F_{\rm III(inv)}$ in F can be neglected in computing A, since neither has spin-one poles at both $\alpha_{12}=1$ and $\alpha_{78}=1$, and hence neither

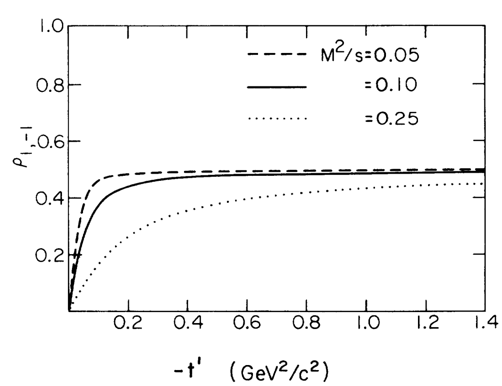

FIG. 5. $\rho_{1,-1}$ in Gottfried-Jackson frame at M^2/s =0.05, 0.1, 0.25.

can contribute to A. Consequently, we can write

$$A'' = F_{\rm I} + F_{\rm I(inv)} + 2F_{\rm II}. \tag{3.3}$$

To obtain A from A'' we proceed as before: Take the residue at the $\alpha_{12}=1$, $\alpha_{78}=1$ poles, eliminate the spin-zero daughter contributions, and factor off the $\rho\pi\pi$ vertices. This yields

$$A = A_{\rm I} + A_{\rm I(inv)} + 2A_{\rm II}, \tag{3.4}$$

where

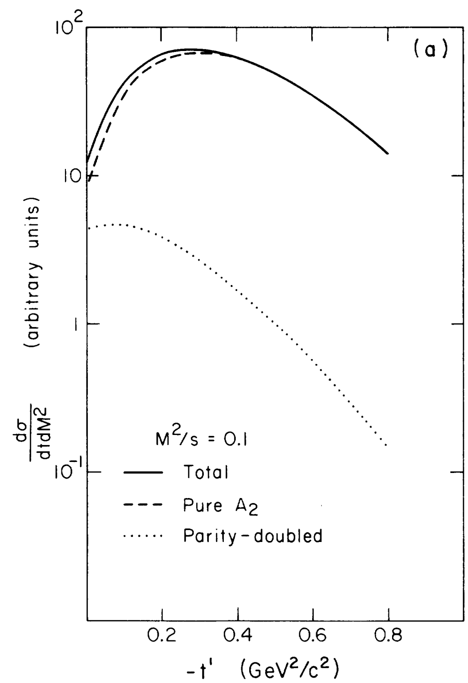

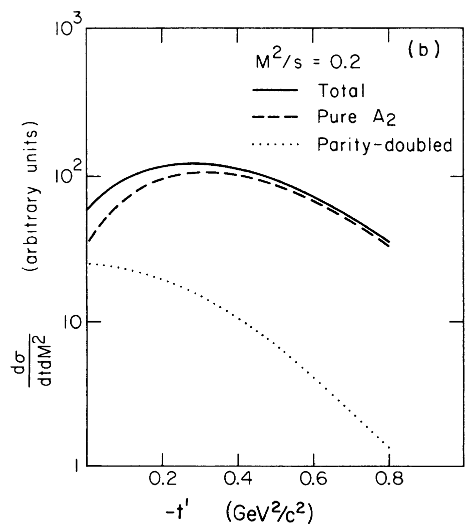

FIG. 6. (a) Pure A_2 versus parity-doubled contributions to $d\sigma/dt\,dM^2$ at $M^2/s=0.1$. (b) Pure A_2 versus parity-doubled contributions at $M^2/s=0.2$.

$$
\begin{aligned}
A_{\mathrm{I}} = (-\alpha'^2)\alpha_{b\bar{b}}\epsilon'^* \cdot p_{\bar{a}}\{ & \epsilon \cdot p_a B_6(\alpha_{a\bar{x}}, \alpha - 1, \alpha_{\bar{a}x}, \alpha_{ab} - 1, \alpha_{ab\bar{b}}, \alpha_{x\bar{x}} - 1, \alpha_{b\bar{b}}, \alpha_{\bar{a}b\bar{b}} - 1, \alpha_{\bar{a}\bar{b}} - 2) \\
& + \epsilon \cdot p_b B_6(\alpha_{a\bar{x}} - 1, \alpha - 1, \alpha_{\bar{a}x}, \alpha_{ab} - 1, \alpha_{ab\bar{b}}, \alpha_{x\bar{x}} - 1, \alpha_{b\bar{b}}, \alpha_{\bar{a}b\bar{b}} - 1, \alpha_{\bar{a}\bar{b}} - 2) \\
& + \epsilon \cdot p_{\bar{b}} B_6(\alpha_{a\bar{x}} - 1, \alpha - 2, \alpha_{\bar{a}x}, \alpha_{ab} - 1, \alpha_{ab\bar{b}}, \alpha_{x\bar{x}} - 1, \alpha_{b\bar{b}}, \alpha_{\bar{a}b\bar{b}} - 1, \alpha_{\bar{a}\bar{b}} - 2) \\
& + \epsilon \cdot p_{\bar{a}} B_6(\alpha_{a\bar{x}} - 1, \alpha - 2, \alpha_{\bar{a}x} - 1, \alpha_{ab} - 1, \alpha_{ab\bar{b}}, \alpha_{x\bar{x}} - 1, \alpha_{b\bar{b}}, \alpha_{\bar{a}b\bar{b}} - 1, \alpha_{\bar{a}\bar{b}} - 2)\}
\end{aligned}
\tag{3.5}
$$

and

$$
A_{\mathrm{II}} = (-\alpha'^2)\alpha\epsilon \cdot p_a\epsilon'^* \cdot p_{\bar{a}} B_6(\alpha_{a\bar{x}}, \alpha, \alpha_{\bar{a}x}, \alpha_{ab} - 1, \alpha_{ab\bar{b}} - 2, \alpha_{x\bar{x}} - 3, \alpha_{b\bar{b}} - 1, \alpha_{\bar{a}b\bar{b}} - 2, \alpha_{\bar{a}\bar{b}} - 1). \tag{3.6}
$$

One obtains $A_{\mathrm{I(inv)}}$ by the substitution

$$(\epsilon, \epsilon'^*, a, b, x, \bar{a}, \bar{b}, \bar{x}) \to (\epsilon'^*, \epsilon, \bar{a}, \bar{b}, \bar{x}, a, b, x)$$

in the expression for A_{I}. Taking the discontinuity one obtains

$$
\begin{aligned}
\left(-\frac{1}{\pi\alpha'^2}\right)\mathrm{Disc}_{M^2}A = & -2\epsilon \cdot p_a\epsilon'^* \cdot p_a(\alpha - 1)\left(\frac{(\alpha_{ab} - 1)(\alpha_{ab} - 2)}{(\alpha - 1)^2}\right)^{\alpha_{a\bar{x}}} I\left(\frac{\alpha - 1}{\alpha_{ab} - 1}, \frac{\alpha - 1}{\alpha_{ab} - 2}; \alpha_{a\bar{x}}, \alpha_{a\bar{x}}, \alpha_{a\bar{x}} + 1, \alpha_{a\bar{x}}, -2, 1\right) \\
& + (\epsilon \cdot p_b\epsilon'^* \cdot p_a + \epsilon \cdot p_a\epsilon'^* \cdot p_b)(\alpha_{ab} - 2)\left(\frac{(\alpha_{ab} - 2)(\alpha_{ab} - 1)}{(\alpha - 1)^2}\right)^{\alpha_{a\bar{x}} - 1} \\
& \times DI\left(\frac{\alpha - 1}{\alpha_{ab} - 2}, \frac{\alpha - 1}{\alpha_{ab} - 1}; \alpha_{a\bar{x}}, \alpha_{a\bar{x}} - 1, \alpha_{a\bar{x}}, \alpha_{a\bar{x}} - 2, 1\right) \\
& + 2\epsilon \cdot p_a\epsilon'^* \cdot p_a(\alpha - 2)\left(\frac{(\alpha_{ab} - 1)(\alpha_{ab} - 2)}{(\alpha - 2)^2}\right)^{\alpha_{a\bar{x}} - 1} \\
& \times I\left(\frac{\alpha - 2}{\alpha_{ab} - 1}, \frac{\alpha - 2}{\alpha_{ab} - 2}; \alpha_{a\bar{x}} - 1, \alpha_{a\bar{x}} - 1, \alpha_{a\bar{x}}, \alpha_{a\bar{x}} - 1, -2, 1\right) \\
& - 2\epsilon \cdot p_a\epsilon'^* \cdot p_a\alpha\left(\frac{\alpha_{ab} - 1}{\alpha}\right)^{2\alpha_{a\bar{x}}} I\left(\frac{\alpha}{\alpha_{ab} - 1}, \frac{\alpha}{\alpha_{ab} - 1}; \alpha_{a\bar{x}}, \alpha_{a\bar{x}}, \alpha_{a\bar{x}}, \alpha_{a\bar{x}}, -2, 0\right).
\end{aligned}
\tag{3.7}
$$

All two- and four-pion channels contain the ρ trajectory except channels with vacuum quantum numbers, in which we use $\alpha_{\mathrm{vac}}(0) = 1$. Three-pion channels contain the pion trajectory. Expressions for the discontinuity in the other terms are found in Table III. The functions B_{fore} and D_{fore} in Table III are used to denote respectively the $(B + C)$ and D obtained using an unmodified B_8 instead of F. The expressions are lengthy and are found in Ref. 1.

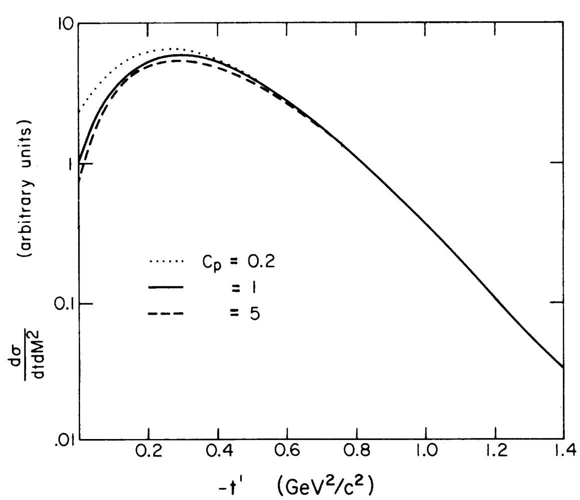

FIG. 7. Comparison of predictions for $c_p = 0.2$, 1, 5, where c_p is the coefficient of the most important term in the amplitude.

C. Results

Numerical evaluation now takes place as before. Figures 9, 10, and 11 display respectively the t' dependence of $d\sigma/dt\,dM^2$, the $p_\perp$ distribution of $E_x d^3\sigma/dp_x{}^3$, and the t' dependence of the density-matrix elements. Results here are less satisfactory than in the abnormal-coupling case and the simpler normal-coupling calculation of Ref. 1. The cancellation problem encountered in Ref. 1 is even worse now. That problem is that near the dip at $t = -1$ $(\mathrm{GeV}/c)^2$ cancellation occurs among the terms leading in s and M^2; and since we neglected nonleading terms the results are unreliable

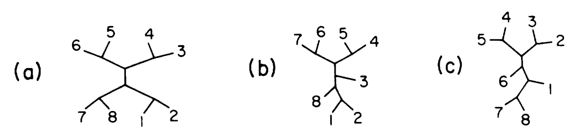

FIG. 8. The tree graphs not covered by the amplitude for normally coupled physical trajectories.

TABLE III. Expressions for Disc_{M^2} of the terms B, C, and D for normally coupled internal trajectories.

$$\mathrm{Disc}_{M^2}(B+C)=\sum_{i=1}^{6} B_i$$

$$B_1=\mathrm{Disc}_{M^2}B_{\mathrm{fore}}(\alpha_{a\bar x},\ \alpha-1,\ \alpha_{\bar a x},\ \alpha_{ab}-1,\ \alpha_{b\bar b},\ \alpha_{\bar b x}-1,\ \alpha_{\bar a x\bar x},\ \text{[illegible]}-1,\ \alpha_{\bar a\bar x})$$

$$B_2=-4\alpha'^2\epsilon\cdot p_a\,\epsilon'^*\cdot p_a\cos(\pi\alpha_{a\bar x})\alpha\pi\Bigg[\left(\frac{\alpha_{ab}-1}{\alpha}\right)^{\alpha_{a\bar x}}\left(-\frac{\alpha_{b\bar x}}{\alpha}\right)^{\alpha_{a\bar x}-1}$$
$$\times I\left(\frac{\alpha}{\alpha_{ab}-1},\ \frac{\alpha}{\alpha_{b\bar x}};\ \alpha_{a\bar x},\ \alpha_{a\bar x}-1,\ \alpha_{a\bar x}+\alpha_{a\,\text{[illegible]}}\ 2,\ \alpha_{\bar a x}+\alpha_{\bar a\bar x},\ -\alpha_{\bar a\bar x}-1,\ 0\right)$$
$$-\left(\frac{(\alpha_{ab}-1)(-\alpha_{b\bar x})}{\alpha^2}\right)^{\alpha_{a\bar x}}I\left(\frac{\alpha}{\alpha_{ab}-1},\ \frac{\alpha}{\alpha_{b\bar x}};\ \alpha_{a\bar x},\ \alpha_{a\bar x},\ \alpha_{a\bar x}+\alpha_{ax}-2,\ \alpha_{a\bar x}+\alpha_{ax},\ -\alpha_{ax},\ 0\right)\Bigg]$$

$$B_3=-2\alpha'^2\alpha\pi\,(\epsilon\cdot p_a\,\epsilon'^*\cdot p_b\,e^{-i\pi\alpha_{a\bar x}}+\epsilon\cdot p_b\,\epsilon'^*\cdot p_a\,e^{i\pi\alpha_{a\bar x}})\left(\frac{\alpha_{ab}-1}{\alpha}\right)^{\alpha_{a\bar x}}\left(-\frac{\alpha_{b\bar x}}{\alpha}\right)^{\alpha_{a\bar x}-1}$$
$$\times DI\left(\frac{\alpha}{\alpha_{ab}-1},\ \frac{\alpha}{\alpha_{b\bar x}};\ \alpha_{a\bar x},\ \alpha_{a\bar x}-1,\ \alpha_{a\bar x}+\alpha_{ax}-2,\ \alpha_{a\bar x}+\alpha_{ax},\ -\alpha_{ax},\ 0\right)$$

$$B_4=\alpha'^2\pi\alpha_{ab}\,\epsilon'^*\cdot p_b\,\epsilon\cdot p_b\,[2\cos(\pi\alpha_{a\bar x})]\left(\frac{\alpha_{ab}}{\alpha-1}\right)^{\alpha_{a\bar x}-2}\left(-\frac{\alpha_{b\bar x}}{\alpha-1}\right)^{\alpha_{a\bar x}-1}$$
$$\times\Bigg[DI\left(\frac{\alpha-1}{\alpha_{ab}},\ \frac{\alpha-1}{\alpha_{b\bar x}};\ \alpha_{a\bar x}-2,\ \alpha_{a\bar x}-1,\ \alpha_{a\bar x}+\alpha_{ax}-2,\ \alpha_{a\bar x}+\alpha_{ax},\ -\alpha_{ax},\ 0\right)$$
$$-\left(\frac{\alpha-1}{\alpha-2}\right)^{2\alpha_{a\bar x}-3}DI\left(\frac{\alpha-2}{\alpha_{ab}},\ \frac{\alpha-2}{\alpha_{b\bar x}};\ \alpha_{a\bar x}-2,\ \alpha_{a\bar x}-1,\ \alpha_{a\bar x}+\alpha_{ax}-2,\ \alpha_{a\bar x}+\alpha_{ax},\ -\alpha_{ax},\ 0\right)\Bigg]$$

$$B_5=-\alpha'^2\alpha_{ab}\pi(\epsilon\cdot p_a\,\epsilon'^*\cdot p_b\,e^{-i\pi\alpha_{a\bar x}}+\epsilon\cdot p_b\,\epsilon'^*\cdot p_a\,e^{+i\pi\alpha_{a\bar x}})\left(-\frac{\alpha_{b\bar x}\alpha_{ab}}{(\alpha-1)^2}\right)^{\alpha_{a\bar x}-1}$$
$$\times DI\left(\frac{\alpha-1}{\alpha_{ab}},\ \frac{\alpha-1}{\alpha_{b\bar x}};\ \alpha_{a\bar x}-1,\ \alpha_{a\bar x}-1,\ \alpha_{a\bar x}+\alpha_{ax}-1,\ \alpha_{a\bar x}+\alpha_{ax},\ -\alpha_{ax},\ 0\right)$$

$$B_6=2\pi\alpha'^2(\alpha-1)\cos(\pi\alpha_{a\bar x})\epsilon\cdot p_a\,\epsilon'^*\cdot p_a\left(\frac{(-\alpha_{b\bar x}+2)(\alpha_{ab}-2)}{(\alpha-1)^2}\right)^{\alpha_{a\bar x}}$$
$$\times I\left(\frac{\alpha-1}{\alpha_{ab}-2},\ \frac{\alpha-1}{\alpha_{b\bar x}-2};\ \alpha_{a\bar x},\ \alpha_{a\bar x},\ \alpha_{a\bar x}+\alpha_{ax}-2,\ \alpha_{a\bar x}+\alpha_{ax}-1,\ -\alpha_{ax},\ 1\right)$$

$$\mathrm{Disc}_{M^2}D=D_1+D_2+D_3$$

$$D_1=2\alpha\,\mathrm{Disc}_{M^2}D_{\mathrm{fore}}(\alpha_{a\bar x},\ \alpha,\ \alpha_{\bar a x},\ \alpha_{b\bar x},\ \alpha_{a\bar a x}-1,\ \alpha_{a\bar a}-1,\ \alpha_{b\bar b}-1,\ \alpha_{a\bar a\bar x}-1,\ \alpha_{\bar b x})$$

$$D_2=+\alpha'^2\pi\epsilon'^*\cdot p_a\Bigg[\epsilon\cdot p_a(\alpha-1)\left(\frac{(\alpha_{b\bar x}-1)(\alpha_{b\bar x}-2)}{(\alpha-1)^2}\right)^{\alpha_{a\bar x}}I\left(\frac{\alpha-1}{\alpha_{b\bar x}-1},\ \frac{\alpha-1}{\alpha_{b\bar x}-2};\ \alpha_{a\bar x},\ \alpha_{a\bar x},\ \alpha_{a\bar x},\ \alpha_{a\bar x},\ -1,\ 1\right)$$
$$-\epsilon\cdot p_a(-\alpha_{b\bar x}+2)\left(\frac{(\alpha_{b\bar x}-1)(\alpha_{b\bar x}-2)}{(\alpha-1)^2}\right)^{\alpha_{a\bar x}-1}I\left(\frac{\alpha-1}{\alpha_{b\bar x}-1},\ \frac{\alpha-1}{\alpha_{b\bar x}-2};\ \alpha_{a\bar x}-1,\ \alpha_{a\bar x},\ \alpha_{a\bar x}-1,\ \alpha_{a\bar x},\ -1,\ 1\right)$$
$$-\epsilon\cdot p_b\left(-\frac{\alpha_{b\bar x}-1}{\alpha-1}\right)^{\alpha_{a\bar x}-1}\left(-\frac{\alpha_{b\bar x}-2}{\alpha-1}\right)^{\alpha_{a\bar x}}I\left(\frac{\alpha-1}{\alpha_{b\bar x}-1},\ \frac{\alpha-1}{\alpha_{b\bar x}-2};\ \alpha_{a\bar x}-1,\ \alpha_{a\bar x},\ \alpha_{a\bar x},\ \alpha_{a\bar x},\ -1,\ 0\right)\Bigg]$$

$$D_3=\alpha'^2\pi\epsilon\cdot p_a\Bigg[\epsilon'^*\cdot p_a(\alpha-1)\left(\frac{(\alpha_{b\bar x}-2)(\alpha_{b\bar x}-1)}{(\alpha-1)^2}\right)^{\alpha_{a\bar x}}I\left(\frac{\alpha-1}{\alpha_{b\bar x}-2},\ \frac{\alpha-1}{\alpha_{b\bar x}-1};\ \alpha_{a\bar x},\ \alpha_{a\bar x},\ \alpha_{a\bar x},\ \alpha_{a\bar x},\ -1,\ 1\right)$$
$$-\epsilon'^*\cdot p_a(-\alpha_{b\bar x}+2)\left(\frac{(\alpha_{b\bar x}-2)(\alpha_{b\bar x}-1)}{(\alpha-1)^2}\right)^{\alpha_{a\bar x}-1}I\left(\frac{\alpha-1}{\alpha_{b\bar x}-2},\frac{\alpha-1}{\alpha_{b\bar x}-1};\ \alpha_{a\bar x},\ \alpha_{a\bar x}-1,\ \alpha_{a\bar x},\ \alpha_{a\bar x}-1,\ -1,\ 1\right)$$
$$-\epsilon'^*\cdot p_b\left(-\frac{\alpha_{b\bar x}-2}{\alpha-1}\right)^{\alpha_{a\bar x}}\left(-\frac{\alpha_{b\bar x}-1}{\alpha-1}\right)^{\alpha_{a\bar x}-1}I\left(\frac{\alpha-1}{\alpha_{b\bar x}-2},\ \frac{\alpha-1}{\alpha_{b\bar x}-1};\ \alpha_{a\bar x},\ \alpha_{a\bar x}-1,\ \alpha_{a\bar x},\ \alpha_{a\bar x},\ -1,\ 0\right)\Bigg]$$

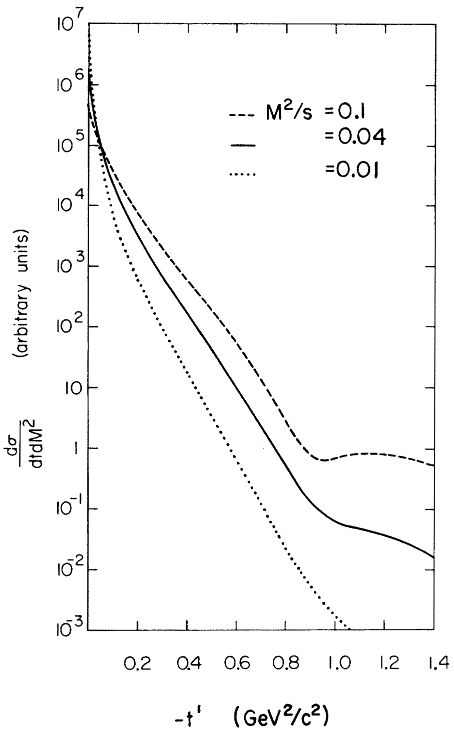

FIG. 9. $d\sigma/dtdM^2$ for π exchange at $M^2/s = 0.1$, 0.04, 0.01.

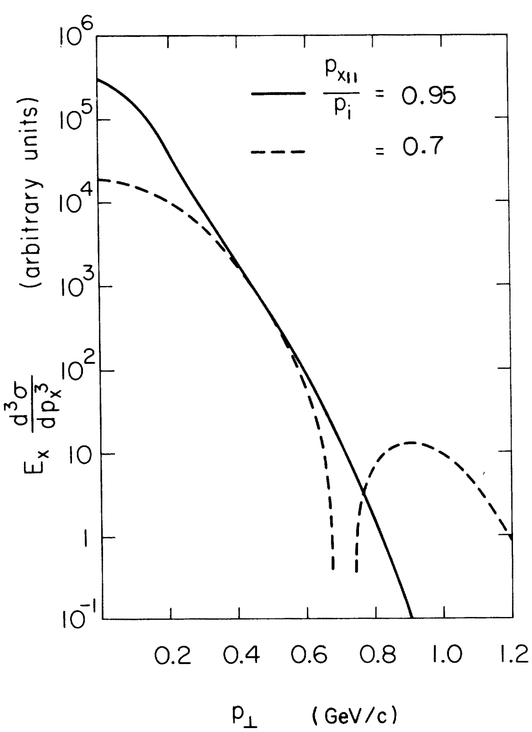

FIG. 10. $E_x d^3\sigma/dp_x{}^3$ for π exchange at $p_{x\parallel}/p_i = 0.95$, 0.7.

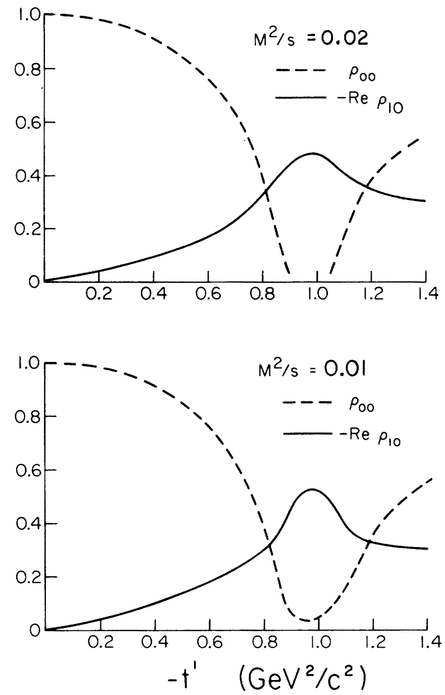

FIG. 11. ρ_{00} and $\mathrm{Re}\rho_{10}$ in the Gottfried-Jackson frame at $M^2/s = 0.01$, 0.02.

when these smaller terms are important, as they are in the vicinity of the dip. This shows up in our results as unphysical values for the density-matrix element ρ_{00}. Comparing these results of the modified amplitude for normal coupling to the results of the previous analysis, using an unmodified B_8, indicates that the results are quite similar qualitatively, the main difference being that in the modified calculation the dip structure develops at smaller values of M^2/s than it did in the original calculation. The similarity of the two sets of results for vector-meson production is to be expected since we have not altered the trajectory in the t channel.

IV. PHYSICAL TRAJECTORIES IN $\pi\pi \to \pi X$

A. Calculation

We are also in a position to study a DRM with physical trajectories in inclusive reactions with a pseudoscalar meson as the observed particle in the final state. These results can then be compared to those of a DRM with unphysical trajectories. A substantial change can be expected in the t' distribution, since we are in effect changing the trajectory in the t channel from a π to a ρ when we include physical trajectories.

For the amplitude we take the six-point amplitude of Ref. 4 and symmetrize it under inversion of ordering of external particles. The symmetrized amplitude is

$$F_6=\alpha_{12}\alpha_{45}B_6(\alpha_{12},\alpha_{13},\alpha_{14}-1,\alpha_{23}-1,\alpha_{24}-1,\ \alpha_{25}-1,\ \alpha_{34}-1,\alpha_{35},\alpha_{45})$$
$$+\alpha_{56}\alpha_{23}B_6(\alpha_{12}-1,\alpha_{13},\alpha_{14},\alpha_{23},\alpha_{24},\alpha_{25}-1,\ \alpha_{34}-1,\alpha_{35}-1,\alpha_{45}-1). \qquad (4.1)$$

We can now take the discontinuity for the four orderings of particles (A,B,C,D) and we obtain

$$\mathrm{Disc}_{M^2}A=-2\pi\alpha_{a\bar{x}}\alpha_{ab}\left(\frac{\alpha_{ab}}{\alpha}\right)^{\alpha_{a\bar{x}}-1}\left(\frac{\alpha_{ab}-1}{\alpha}\right)^{\alpha_{a\bar{x}}}I\left(\frac{\alpha}{\alpha_{ab}-1},\frac{\alpha}{\alpha_{ab}};\alpha_{a\bar{x}},\alpha_{a\bar{x}},\alpha_{a\bar{x}}-1,\alpha_{a\bar{x}},\alpha_{a\bar{x}}+1,-2,0\right), \qquad (4.2)$$

$$\mathrm{Disc}_{M^2}(B+C)=-2\pi\alpha_{a\bar{x}}\alpha\cos(\pi\alpha_{a\bar{x}})\left(\frac{\alpha_{ab}(-\alpha_{b\bar{x}}+1)}{\alpha^2}\right)^{\alpha_{a\bar{x}}}$$
$$\times I\left(\frac{\alpha}{\alpha_{b\bar{x}}-1},\frac{\alpha}{\alpha_{ab}};\alpha_{a\bar{x}},\alpha_{a\bar{x}}-1,\alpha_{a\bar{x}}+\alpha_{ax}-1,\alpha_{a\bar{x}}+\alpha_{ax},-\alpha_{ax}-1,0\right)$$
$$-2\pi\alpha_{a\bar{x}}\alpha\cos(\pi\alpha_{a\bar{x}})\left(\frac{-\alpha_{b\bar{x}}(\alpha_{ab}-1)}{\alpha^2}\right)^{\alpha_{a\bar{x}}}$$
$$\times I\left(\frac{\alpha}{\alpha_{b\bar{x}}},\frac{\alpha}{\alpha_{ab}-1};\alpha_{a\bar{x}}-1,\alpha_{a\bar{x}},\alpha_{a\bar{x}}+\alpha_{ax},\alpha_{a\bar{x}}+\alpha_{ax}-1,-\alpha_{ax}-1,0\right) \qquad (4.3)$$

$$\mathrm{Disc}_{M^2}D=-2\pi\alpha_{a\bar{x}}\alpha\left(\frac{\alpha_{b\bar{x}}(\alpha_{b\bar{x}}-1)}{\alpha^2}\right)^{\alpha_{a\bar{x}}}I\left(\frac{\alpha}{\alpha_{b\bar{x}}-1},\frac{\alpha}{\alpha_{b\bar{x}}};\alpha_{a\bar{x}},\alpha_{a\bar{x}}-1,\alpha_{a\bar{x}},\alpha_{a\bar{x}}+1,-2,0\right). \qquad (4.4)$$

Taking proper account of the Chan-Paton factor[11] to ensure correct signature, we use

$$\frac{1}{\sigma_{ab}}E_x\frac{d^3\sigma}{dp_x{}^3}=\frac{\Gamma(\alpha_{\rm vac}+1)}{\pi\alpha_{ab}{}^{\alpha_{\rm vac}}}\mathrm{Disc}_{M^2}(A-B-C+D). \qquad (4.5)$$

In the numerical evaluation of this we use the ρ in two-π channels, the π in three-π channels, and the simulated Pomeron for our vacuum exchange.

B. Results

The effects of including physical trajectories are greater for production of pseudoscalar mesons than they were for the vector-meson production. In the calculation using an unmodified B_6 the t-channel trajectory was in effect the pion, whereas now we have a ρ trajectory. Figures 12 and 13 point out this difference both in the position of the minimum and in the behavior at small t' (or $p_\perp$), which is not at all the steep exponential of the earlier case. For comparison the two results for $M^2/s=0.2$ are shown in Fig. 14.

V. DISCUSSION AND CONCLUSIONS

DRM calculations are often done using the unmodified B_N in the spirit of trying to abstract from the calculation properties or features which are general features of the DRM and not merely peculiar to the particular amplitude used. Our calculation can serve to demonstrate which features are common to different DRM amplitudes. In this regard, the predictions on the firmest footing are those which would be common to most Regge models. In order to take the discontinuity in M^2, we went to the asymptotic limit in M^2 (and hence s). In doing so we lost some detailed information (such as most of the resonant structure) and are using the DRM primarily as a Regge model with pre-

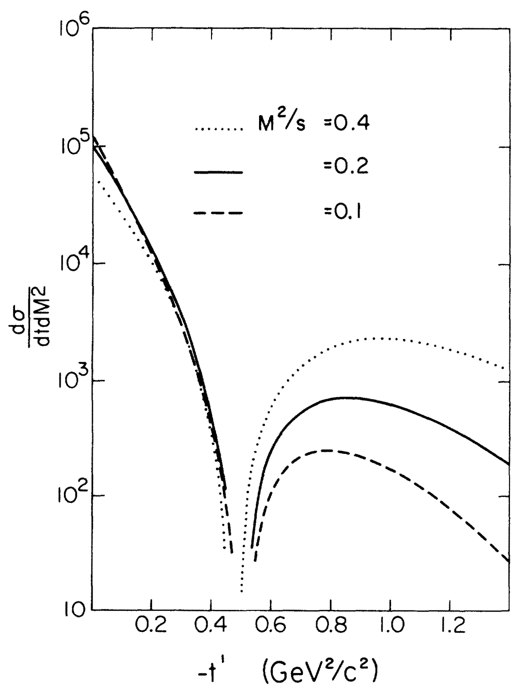

FIG. 12. $d\sigma/dt\,dM^2$ for spinless meson production at $M^2/s=0.4$, 0.2, 0.1.

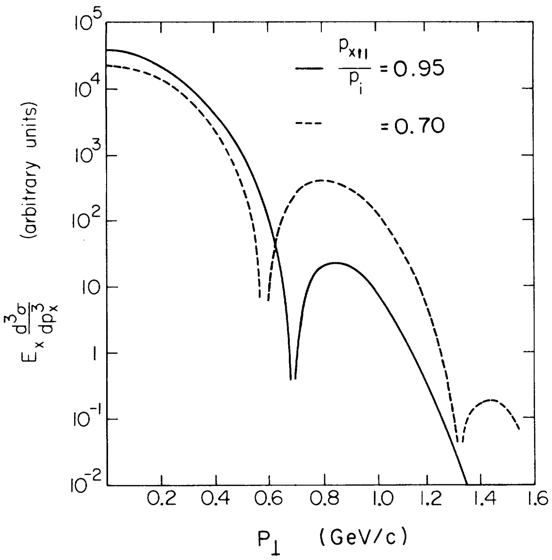

FIG. 13. $E_x d^3\sigma/dp_x^3$ for spinless meson production at $p_{x\parallel}/p_i = 0.95$, 0.7.

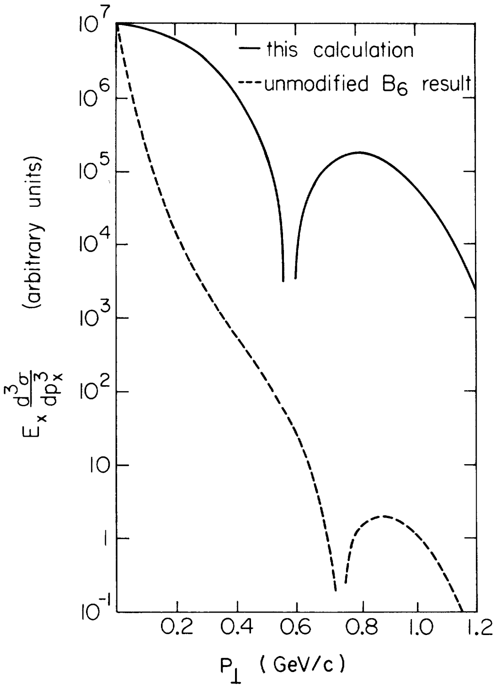

FIG. 14. Comparison of predictions for spinless meson production with and without physical trajectories. (Curves have been normalized to start at same point.) Predictions are for $p_{x\parallel}/p_i = 0.7$.

scribed residues—and, of course, with a definite prescription for handling unstable particles.

The inclusion of positive-intercept trajectories for π exchange in vector-meson production does not lead to any new and interesting behavior. This is due to the fact that the t-channel trajectory (π) was handled satisfactorily in the unmodified B_8. Besides not introducing any new features physically, it does introduce more computational headaches due to its greater complexity and its propensity toward emphasizing the breakdown of our approximations in the dip region. In all fairness it should be mentioned that inclusion of positive-intercept trajectories does allow us to use $\alpha_{vac}(0)=1$, which leads to more reasonable M^2 and s dependence. However, if only $(1/\sigma_{ab})E_x d^3\sigma/dp_x^3$ is considered, as in Ref. 1, this dependence on the vacuum trajectory is effectively removed. It appears than an unmodified B_8 is preferable for vector-meson production since it contains all the main features and is easier to work with.

For the production of pseudoscalar mesons, the situation is different. Now inclusion of positive intercepts allows us to put a realistic ρ trajectory in the t channel instead of the hybrid π-ρ used before. This affects the position of the minimum and also the slope in the forward direction. When comparison to data is intended, the modified B_6 with physical trajectories should be used for the one-particle spectrum if we are going to be fair to the DRM. Its use is no more difficult than that of the unmodified B_6.

For abnormal coupling (A_2 exchange in ρ production), simple kinematics force us to use a relatively complicated model. The amplitude we used was highly nonunique; however, most of the general features are expected from any Regge model and therefore are not peculiar to our choice of an amplitude.

Clearly any attempt to study the production (inclusive or exclusive) of spinning particles must allow for different types of exchanges. As can be seen from our calculations, the "hallmarks" of particular quantum-number exchange, such as dips and relations between density-matrix elements, carry over fairly closely from the exclusive to the inclusive case. One must be prepared to devote the same attention to kinematics as in the exclusive case if any serious study of reaction mechanisms is to be attempted.

Present data for exclusive ρ production in charge-exchange reactions do not show any appreciable A_2-exchange contributions.[12] Because the A_2 trajectory is higher than the π trajectory, the A_2 should dominate at sufficiently high energy. The large coupling of the pion to the $\rho\pi$ and to the $p\bar{n}$, however, requires that the energy be very high before the A_2 finally gains the upper hand. The situation may be better in inclusive reactions. The reason for this is that instead of a $\pi p\bar{n}$ vertex versus an $A_2 p\bar{n}$ vertex, we will have the π and A_2 total (off-shell) cross sections on protons. If the ratio of these is not so large as the ratio of their respective (squared) couplings to $p\bar{n}$, the A_2 would make its presence felt earlier.

Counterbalancing this there is a drawback of looking for the A_2 exchange in inclusive reactions. This is the fact that the quantity which must be large for A_2 to dominate over π exchange is s/M^2, where M^2 is the missing mass squared. If we need to go to large M^2 before $\sigma^{\rm tot}_{A_2N}(M^2)/\sigma^{\rm tot}_{\pi N}(M^2)$ (for off-shell π and A_2) becomes appreciably larger than it is at $M^2 \sim 1$ GeV^2, then we will have to go to a correspondingly higher value of s to maintain the value of M^2/s which will assure A_2 dominance (or competitiveness). If the gain discussed in the previous paragraph can more than offset this, then the A_2-exchange contribution should become noticeable at a lower *incident energy* in inclusive reactions than in exclusive reactions. And as we have seen in our model calculations, the presence of an appreciable A_2-exchange contribution should be detectable just from the shape of the differential cross section—particularly at smaller values of M^2.

Distributions in the central region would be desirable. The present absence of these distributions is mitigated somewhat by the fact that on the basis of what has been done we have a good idea of what the central-region predictions must be. For A_2 exchange, the density matrix elements ρ_{11} and $\rho_{1\,-1}$ both stay constant at 0.5. The cross section continues to decrease, but becomes a little flatter. The small bumps die away. For π exchange, the situation is similar to that of Ref. 1. As $|t'|$ increases, ρ_{00} increases to a value consistent with the results of Fenster and Uretsky[13] and Kang and Shen.[14] For ρ exchange in π production, the results should be similar to those of DKTW.[8] Only one ordering survives in the central region and our modified amplitude has essentially the same asymptotic behavior (as $s, M^2, |t|, |u| \to \infty$) as their amplitude for this ordering of external particles, the difference being that our vacuum trajectory has intercept unity. But they found this intercept to have small effect on the t or $p_\perp$ distributions.

ACKNOWLEDGMENT

The author is grateful to Professor Lorella M. Jones for numerous helpful suggestions and illuminating discussions. He also acknowledges a helpful conversation with Dr. M. Jacobs.

*Work supported in part by the National Science Foundation under Grant No. NSF GP 25303.

†Present address: Physics Department, Texas A&M University, College Station, Texas 77843.

[1] J. Randa, Phys. Rev. D 7, 2236 (1973).

[2] Chan Hong-Mo and Tsou Sheung-Tsun, Phys. Lett. 28B, 485 (1968).

[3] Gerald P. Canning and Matthew A. Jacobs, (a) Phys. Rev. D 3, 891 (1971); (b) *ibid.* 3, 1928 (1971).

[4] V. Rittenberg and H. R. Rubinstein, Phys. Rev. Lett. 25, 191 (1970).

[5] Chan Hong-Mo, Phys. Lett. 28B, 425 (1969); Chan Hong-Mo and J. F. L. Hopkinson, Nucl. Phys. B14, 28 (1969); Z. Koba and H. B. Nielsen, *ibid.* B10, 633 (1969).

[6] K. Bardakci and H. Ruegg, Phys. Lett. 28B, 671 (1969).

[7] J. D. Dorren, V. Rittenberg, H. R. Rubinstein, M. Chaichian, and E. J. Squires, Nuovo Cimento 1A, 149 (1971).

[8] C. E. DeTar, Kyungsik Kang, Chung-I Tan, and J. H. Weis, Phys. Rev. D 4, 425 (1971).

[9] Lorella Jones, Phys. Rev. 163, 1523 (1967).

[10] C. Lovelace, Phys. Lett. 28B, 264 (1968).

[11] J. E. Paton and Chan Hong-Mo, Nucl. Phys. B10, 516 (1969).

[12] P. Baillon *et al.*, Phys. Lett. 35B, 453 (1971); J. Bartsch *et al.*, Nucl. Phys. B46, 46 (1972); F. Bulos *et al.*, Phys. Rev. Lett. 26, 1453 (1971).

[13] S. Fenster and J. L. Uretsky, Phys. Rev. D 7, 2143 (1973).

[14] Kyungsik Kang and Pu Shen, Phys. Rev. D 7, 164 (1973).